

Exact Quadrature of Singular and Nearly Singular Potential Integrals

*Original*

Exact Quadrature of Singular and Nearly Singular Potential Integrals / Graglia, Roberto; Lombardi, Guido. - ELETTRONICO. - 1:(2007), pp. 982-985. (Intervento presentato al convegno International Conference on Electromagnetics in Advanced Applications tenutosi a Torino (Italy) nel September 17-21, 2007) [10.1109/ICEAA.2007.4387471].

*Availability:*

This version is available at: 11583/1662335 since:

*Publisher:*

IEEE

*Published*

DOI:10.1109/ICEAA.2007.4387471

*Terms of use:*

This article is made available under terms and conditions as specified in the corresponding bibliographic description in the repository

*Publisher copyright*

(Article begins on next page)

# Exact Quadrature of Singular and Nearly Singular Potential Integrals

R. D. Graglia\*

G. Lombardi†

**Abstract** — This paper describes a new numerical technique based on the cancellation method to compute singular and nearly singular potential integrals with machine precision.

## 1 Introduction

The numerical evaluation of multiple integrals with singular kernels is a necessary part of the moment-method solution of electromagnetic problems formulated in terms of integral equations. Self-term integrals are obtained for coincident source and testing domains; near-self integrals occur whenever the source and the testing domains are very close to each other, but do not overlap. In the self-term case, the singular point of the integral kernel belongs to the integration region whereas, in the near-self case, the integration region does not contain the singular point. In spite of the fact that the singularity of the integral kernel is not encountered in the near-self case, the accurate evaluation of these integrals is often more difficult than in the self-term case. Important results for the numerical computation of multiple integrals involving the three-dimensional Greens function and its gradient have already been published [1], [2], [3], [4].

Modern electromagnetic (EM) codes model the geometry of a given problem as the union of sub-domains of different but simple geometrical shape. EM problems are then numerically solved by expanding the unknowns in terms of vector or scalar functions locally defined on these sub-domains. The expansion functions are conveniently defined on rectilinear domains of a *parent* space, with all sub-domains of the global geometry obtained by properly mapping one or few parent domains into the global object-space. In its parent space a domain is described in terms of normalized (dimensionless) parent coordinates, and the parent domain is rectilinear although the corresponding object-space sub-domains could be curvilinear. The word *element* indicates a sub-domain together with a set

of expansion functions defined over there, and associated with a certain number of degrees of freedom. Several elements were defined and used in previous works. Two-dimensional (2D) triangular and quadrilateral elements, as well as three-dimensional (3D) tetrahedral and brick elements are for example discussed in [5], whereas prism and pyramidal elements are given in [6] and [7], respectively. In the following we assume the reader to be comfortable with the definitions given in those papers, and adopt the same notation used there to present a new application of the singularity *cancellation method* to evaluate potential integrals. The cancellation method is based on variable transformations whose Jacobian cancels out the singularity of the kernel of the potential integral. The superiority of the cancellation method with respect to other methods is discussed, for example, in [4].

Our new technique to compute singular and nearly singular potential integrals is described in detail in [8], where we also provide the rules to establish the quadrature weights/points (including their number) to guarantee machine precision. The integration scheme is based on a new rational expression of the singular and nearly singular integrals obtained by special variable transformations and quadratures: Gauss quadrature for rational functions [9], together with classical Gauss-Legendre quadrature. The technique can deal with static and dynamic potentials on surface and volume elements. In particular, in the static case of polynomial source distributions the new cancellation procedure allows for the exact integration of the potential integrals.

Preliminary results of this work have been presented in [10]; in this paper, for the sake of brevity, we focus our discussion on the general procedure to obtain the variable transformation formulas required for singularity cancellation. Several numerical results for potential integrals will be presented at the conference.

## 2 The cancellation technique

Potential integrals on a given element are normally evaluated by subdividing the element region in the object-space into sub-domains, obtained by joining with a line each vertex of the entire domain to the

\*Dipartimento di Elettronica, Politecnico di Torino, C.so Duca degli Abruzzi 24, 10129 Torino, Italy, e-mail: roberto.graglia@polito.it, tel.: +39 011 564000, fax: +39 011 5644099.

†Dipartimento di Elettronica, Politecnico di Torino, C.so Duca degli Abruzzi 24, 10129 Torino, Italy, e-mail: guido.lombardi@polito.it, tel.: +39 011 564000, fax: +39 011 5644099.

given observation point  $\mathbf{r}$ . Subdivision requires element sub-meshing driven by the observation point, and re-parameterization of each sub-domain with a parent sub-mapping in terms of parent coordinates. We assume that the expansion functions are given in terms of the parent coordinates of the entire element, where each element is described by a set  $\boldsymbol{\xi}$  of normalized parametric coordinates  $\boldsymbol{\xi} = (\xi_1, \xi_2, \dots, \xi_\sigma)$ . These are chosen so that the  $i$ -th edge of a two-dimensional element, or the  $i$ -th face of a three-dimensional element, is the zero-coordinate surface for the normalized coordinate  $\xi_i$ . Two coordinates on 2D, and three coordinates on 3D elements are then selected as independent coordinates, the remaining coordinates become dependent coordinates, and each is related to the independent coordinates via a dependency relation [5]-[7]. All parametric coordinates are positive inside the element, and every point outside of the element has one or more negative parent coordinate. For nested integration over the element region

$$\mathcal{E}_\xi = \{\xi_i \mid \xi_i \geq 0, \forall i \in [1, \sigma]\} \quad (1)$$

the  $\xi$  upper bounds must be obtained explicitly through the dependency relationships, thereby ensuring never negative coordinates within the integration region. The  $\xi$  upper bounds of all the elements given in [5]-[7] are always equal or less than unity, although properly specified by the relevant dependency relationships.

The number  $\sigma$  of parametric coordinates used to describe a given element is the *size* of the element or, that is the same, the size of the set  $\boldsymbol{\xi}$ . Therefore, the size of a two-dimensional element is the number of its edges whereas, for three-dimensional elements, the size  $\sigma$  is given by the number of the element faces. The size of the triangular and quadrilateral element is three and four, respectively; the size of the tetrahedron is four; six is the size of the brick, and five is the size of the triangular-prism and of the pyramid.

In the object space the element geometry is defined by  $n_p$  interpolation (or control) points  $\mathbf{r}_{[I]}$ , where  $[I] = [I_1, I_2, \dots, I_\sigma]$  is a multi-index array of size  $\sigma$ , with integer entries  $I_j \in [0, n_p]$  for  $j = 1, \sigma$ . The element dependency relations give further bounds to the integer entries  $I_j$  of the multi-index array, and these bounds depend on the shape, size and dimension of the element [5]-[7]. The position vector in the object space is then expressed in terms of  $n_p$  shape functions  $P_{[I]}(\boldsymbol{\xi})$ , usually of polynomial form, attached to each interpolation or control point

$$\mathbf{r}(\boldsymbol{\xi}) = \sum_{[I]} \mathbf{r}_{[I]} P_{[I]}(\boldsymbol{\xi}) \quad (2)$$

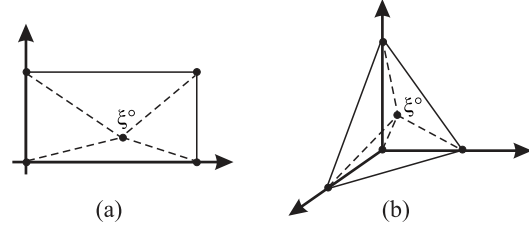


Figure 1: By joining the point  $\boldsymbol{\xi}^\circ = (\xi_1^\circ, \dots, \xi_4^\circ)$  to each domain vertex, a domain of size 4 is subdivided into four triangular (at left) or tetrahedral (at right) sub-domains.

In the global object space, the element region is the whole set of points  $\mathbf{r}(\boldsymbol{\xi})$  obtained by mapping with (2) all the points of the parent region  $\mathcal{E}_\xi$  defined in (1).

For a given element of size  $\sigma$ , a potential integral on  $\boldsymbol{\xi}$  over the element region  $\mathcal{E}_\xi$  is subdivided into  $\sigma$  sub-integrals, with integral subdomains obtained by joining, in the parent space, a point  $\boldsymbol{\xi}^\circ = (\xi_1^\circ, \xi_2^\circ, \dots, \xi_\sigma^\circ)$  to each vertex of the parent domain (see Fig. 1).  $\boldsymbol{\xi}^\circ$  is the arbitrarily located common origin of  $\sigma$  different local pseudo-radial frames introduced to *locally* perform each sub-integral by properly changing the integration variables; the Jacobian of each variable transformation vanishes at  $\boldsymbol{\xi}^\circ$ .

In applications involving 3D elements,  $\boldsymbol{\xi}^\circ$  is the parent point that maps the observation point  $\mathbf{r}$  of the global object-space; notice that in the object space we use no superscript for the observation point  $\mathbf{r}$ , whereas the source (*i.e.*, integration) point  $\mathbf{r}'$  is primed. In applications involving planar 2D elements,  $\boldsymbol{\xi}^\circ$  is the parent point that maps, in the global space, the normal projection  $\mathbf{r}_p$  of the observation point  $\mathbf{r}$  onto the element surface, or onto its extension. If the 2D element is not planar, the 2D potential integrals are performed by working with a rectilinear planar patch of the object space that is tangent to the original curved one; in this case  $\boldsymbol{\xi}^\circ$  is the point that maps the normal projection  $\mathbf{r}_p$  of the observation point  $\mathbf{r}$  onto this tangent patch.

The variable transformation formulas required for singularity cancellation are easily obtained by applying, in the parent space, a general four-step procedure, described in the following paragraphs: 2.1-Duplication of the parent set; 2.2-Introduction of the pseudo-radial variable; 2.3-Radial-binding at observation point  $\boldsymbol{\xi}^\circ$ ; 2.4-Sub-domain selection via zero-blocking and variable transformation formulas.

**2.1. Duplication of the parent set.** Beside the parametric set  $\boldsymbol{\xi}$ , we introduce a second

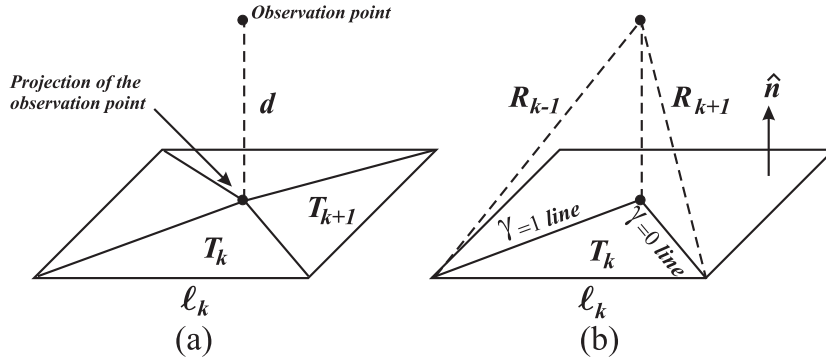


Figure 2: A four-sided planar patch of the object space is broken into four triangular subdomains about the normal projection  $r_p$  of the observation point  $r$  onto the plane of the patch; the distance from  $r$  to the plane of the patch is  $d$ .

set  $\Upsilon$  of normalized coordinates having the same size as  $\xi$ . The  $\Upsilon$ -parametric coordinates satisfy the same dependency relationships that hold for the  $\xi$ -coordinates, and the region  $\mathcal{E}_\Upsilon = \{\Upsilon_i | \Upsilon_i \geq 0, \forall i \in [1, \sigma]\}$  is the duplicate of the whole integration domain  $\mathcal{E}_\xi$ ; in other words, the two sets  $\xi$  and  $\Upsilon$  are equal, but for the name given to the coordinates of each set.

**2.2. Introduction of the pseudo-radial variable.** We introduce a new parametric variable  $\rho \geq 0$ , and then append this variable to the duplicated set  $\Upsilon$  to form the new parametric set  $\Upsilon_\rho = (\Upsilon_1, \Upsilon_2, \dots, \Upsilon_\sigma, \rho)$ , with size equal to  $\sigma + 1$ .

**2.3. Radial-binding at  $\xi^\circ$ .** We bind the  $\xi$  and the  $\Upsilon_\rho$  set together by setting

$$\xi_i = \xi_i^\circ (1 - \rho) + \rho \Upsilon_i, \quad \text{for } i = 1, \sigma \quad (3)$$

so to obtain, for all the allowed values of the integer subscript  $i$  ( $= 1, \sigma$ )

$$\begin{cases} \xi_i = \xi_i^\circ & \text{at } \rho = 0, \\ \xi_i = \Upsilon_i & \text{at } \rho = 1 \end{cases} \quad (4)$$

The pseudo-radial variable  $\rho$  binds the two sets together at  $\xi^\circ$  since, for  $\rho \neq 0$ , eq. (3) requires  $\Upsilon_i = \xi_i^\circ$  whenever  $\xi_i = \xi_i^\circ$ .

**2.4. Subdomain selection via zero-blocking and variable transformation formulas.** By *blocking* to zero one  $\Upsilon$ -coordinate at a time of the augmented set  $\Upsilon_\rho$  one obtains  $\sigma$  different sets of size  $\sigma$  that are used together with (3) to subdivide the original parent domain into  $\sigma$  subdomains. Only the *unblocked* coordinates can vary in a blocked set, although all the coordinates remain bounded by the dependency relationships duplicated in step 2.1. The transformation formulas for integration

on the  $k$ -th subdomain via singularity cancellation are thus simply obtained by setting

$$\Upsilon_k = 0 \quad (5)$$

into (3), for  $k = 1, 2, \dots, \sigma$ . The  $k$ -th subdomain is mapped by the region  $\{\rho \in [0, 1], \Upsilon \in \mathcal{E}_\Upsilon, \text{ with } \Upsilon_k = 0\}$ . The coordinate-surface  $\xi_k = 0$  bounds the  $k$ -th subdomain as well as the entire parent element, because of eqs. (3, 5) and the second of (4), that yields  $\Upsilon_k = \xi_k = 0$  at  $\rho = 1$ .

**2.5. Transformation Jacobians.** The Jacobians of the variable transformation formulas obtained in this manner vanish at  $\rho = 0$ , where the parent integration point  $\xi$  coincides with  $\xi^\circ = (\xi_1^\circ, \xi_2^\circ, \dots, \xi_\sigma^\circ)$ ; this is why  $\rho$  is referred to as a pseudo-radial variable. In particular, for the  $k$ -th subdomain selected by setting  $\Upsilon_k = 0$ , the Jacobian  $\mathcal{J}_k$  becomes  $\mathcal{J}_k = \xi_k^\circ \rho$  in case of 2D elements whereas, for 3D-elements, one has  $\mathcal{J}_k = \xi_k^\circ \rho^2$ .

To exemplify the procedure, let us consider a triangular ( $T$ ) and a quadrilateral ( $Q$ ) element subdivided into triangular subdomains. The procedure maps each sub-domain  $T_k$  into the square domain  $\{\rho \in [0, 1], \Upsilon \in [0, 1]\}$ .

The triangular domain  $T$  is split into three subdomains  $T_k$  ( $k = 1, 2, 3$ ) with subscripts counted modulo three. By setting  $\Upsilon_k = 0$  as per eq. (5), the duplicated dependency relation (see [5])  $\Upsilon_k + \Upsilon_{k+1} + \Upsilon_{k-1} = 1$  yields  $\Upsilon_{k-1} = (1 - \Upsilon_{k+1})$ . In this case, by dropping the subscript in  $\Upsilon_{k+1}$  (that is, by setting  $\Upsilon = \Upsilon_{k+1}$ ), the variable transformation formulas (3) for the  $k$ -th subdomain read as follows

$$\begin{cases} \xi_k = \xi_k^\circ (1 - \rho) \\ \xi_{k+1} = \xi_{k+1}^\circ (1 - \rho) + \rho \Upsilon \\ \xi_{k-1} = \xi_{k-1}^\circ (1 - \rho) + \rho (1 - \Upsilon) \end{cases} \quad (6)$$

For the quadrilateral domain  $Q$  (see Fig. 2), split into four subdomains  $T_k$  ( $k = 1, 2, 3, 4$ ), one counts the subscripts modulo four to write the two dependency relationships  $(\xi_k + \xi_{k+2}) = 1$  and  $(\xi_{k+1} + \xi_{k-1}) = 1$  (see [5]). By setting  $\Upsilon_k = 0$  as per eq. (5), the duplicated dependency relationships yield  $\Upsilon_{k+2} = 1$  and  $\Upsilon_{k-1} = (1 - \Upsilon_{k+1})$ . One then drops the subscript in  $\Upsilon_{k+1}$  and simplifies the transformation formulas (3) for the  $k$ -th subdomain of a quadrilateral as it follows

$$\begin{cases} \xi_k &= \xi_k^\circ (1 - \rho) \\ \xi_{k+2} &= \xi_{k+2}^\circ (1 - \rho) + \rho \\ \xi_{k+1} &= \xi_{k+1}^\circ (1 - \rho) + \rho\Upsilon \\ \xi_{k-1} &= \xi_{k-1}^\circ (1 - \rho) + \rho(1 - \Upsilon) \end{cases} \quad (7)$$

Notice that (6) and (7) fully comply with the dependency relationships of the triangular and quadrilateral element, respectively. Both (6) and (7) can deal with a point  $\xi^\circ$  located outside the parent domain, or on its border.

### 3 Evaluation of the potential integral

The singularity cancellation procedure can be applied, for example, to potential integrals of the form

$$\mathcal{I}_S = \int_S \mathbf{\Lambda}(\mathbf{r}') \frac{\exp(-jkR)}{4\pi R} dS' \quad (8)$$

where  $\mathbf{\Lambda}(\mathbf{r})$  is a vector or scalar basis function,  $\mathbf{R} = \mathbf{r} - \mathbf{r}'$  is the vector distance from observation to integration point, and  $R = |\mathbf{R}|$ . By using successive variable transformations into parent coordinates and then into pseudo-radial coordinates, and by using the modified Euler's substitution given in [8] one gets

$$\mathcal{I}_S = \frac{\mathcal{J}}{4\pi} \sum_k \frac{\xi_k^\circ}{\ell_k} \int_0^1 d\rho \int_0^1 \mathbf{\Lambda}(\rho, \varphi) \frac{\exp(-jkR)}{\varphi - \tilde{\varphi}} d\varphi \quad (9)$$

where  $\mathcal{J}$  is the Jacobian of the transformation between global and parametric  $\xi$ -coordinates, and  $\varphi$  is the new integration variable that has substituted  $\Upsilon$ , and with  $\tilde{\varphi} = -C_k/\rho$ .  $C_k$  is a real function of  $\rho$  that does not depend on  $\varphi$ , with  $C_k > 0$  and  $\tilde{\varphi} < 0$  for all  $\rho$  in the integration interval  $[0, 1]$ . The integral (9) is evaluated numerically by integrating first along  $\varphi$  (using Gauss quadrature for rational functions [9]), that is for  $\rho = \text{const.}$ , and then on  $\rho$  (using Gauss-Legendre quadrature). This integral simplifies considerably when the observation points lies on the patch-surface (self-element integration) or on its extension, that is for  $d = 0$ .

Preliminary results for a right triangle  $T$ , with catheti of 1[m] in length are reported in [10].

### Acknowledgment.

This work is supported by NATO under the grant CBP.MD.SFPP 982376.

### References

- [1] D. R. Wilton, S. M. Rao, A. W. Glisson, D. H. Schaubert, O. M. Al-Bundak, and C. M. Butler, "Potential integrals for uniform and linear source distributions on polygonal and polyhedral domains," *IEEE Trans. Antennas Propag.*, vol. 32, pp. 276-281, Mar. 1984.
- [2] R. D. Graglia, "On the numerical integration of the linear shape functions times the 3-D Greens function or its gradient on a plane triangle," *IEEE Trans. Antennas Propag.*, vol. 41, pp. 1448-1456, Oct. 1993.
- [3] L. Rossi and P. J. Cullen, "On the fully numerical evaluation of the linear-shape function times the 3-D Greens function on a plane triangle," *IEEE Trans. Microwave Theory Tech.*, vol. 47, pp. 398-402, Apr. 1999.
- [4] M. A. Khayat, and D. R. Wilton, "Numerical evaluation of singular and near-singular potential integrals," *IEEE Trans. Antennas Propag.*, vol. 53, pp. 3180-3190, Oct. 2005.
- [5] R.D. Graglia, D.R. Wilton and A.F. Peterson, "Higher order interpolatory vector bases for computational electromagnetics," special issue on "Advanced Numerical Techniques in Electromagnetics" *IEEE Trans. Antennas Propagat.*, vol. 45, no. 3, pp. 329-342, Mar. 1997.
- [6] R.D. Graglia, D.R. Wilton, A.F. Peterson, and I.-L. Gheorma, "Higher order interpolatory vector bases on prism elements," *IEEE Trans. Antennas Propagat.*, vol. 46, no. 3, pp. 442-450, Mar. 1998.
- [7] R. D. Graglia, and I.-L. Gheorma, "Higher order interpolatory vector bases on pyramidal elements," *IEEE Trans. Antennas Propagat.*, vol. 47, no. 5, pp. 775-782, May 1999.
- [8] R. D. Graglia, and G. Lombardi "Machine precision evaluation of singular and nearly singular potential integrals by use of Gauss quadrature formulas for rational functions," *IEEE Trans. Antennas Propag.*, submitted for publication.
- [9] W. Gautschi, "Algorithm 793: GQRAT-Gauss Quadrature for Rational Functions," *ACM Trans. Math. Softw.*, vol. 25, no. 2, pp. 213-239, 1999.
- [10] G. Lombardi, and R. D. Graglia "Accurate evaluation of potential integrals with Gauss quadrature formulas for rational functions," *Proc. of the IEEE AP-S Int. Symp.*, pp. 4841-4844, Honolulu, June 2007.